

## Effect of Diethanolamine (DEA) Solvent Flow Rate on the CO<sub>2</sub> Absorption-Desorption Process Using a Hollow Fiber Membrane Contactor

Raditya Yudhi Pamungkas<sup>a</sup>, Siti Nurkhamidah<sup>a</sup>, Fadlilatul Taufany<sup>a</sup>, Ali Altway<sup>a</sup>, Susianto<sup>a</sup>, Yeni Rahmawati<sup>a\*</sup>

*Department of Chemical Engineering, Faculty of Industrial Technology and Systems Engineering, Institut Teknologi Sepuluh Nopember, Surabaya, East Jawa, 60111, Indonesia*

### Article history:

Submitted 22 June 2025  
Revision 17 July 2025  
Accepted 21 July 2025  
Online 1 August 2025

**ABSTRACT:** One of the primary objectives in decarbonization is the separation of CO<sub>2</sub> from industrial gas mixtures, particularly in application such as biogas purification and flue gas treatment. A dual-layer crossflow membrane module was utilized under both circulation and batch operating modes with a 30% DEA solution. This study investigates the influence of solvent flow velocity on CO<sub>2</sub> separation performance using a hollow fiber membrane contactor with a 30% DEA solvent. The process was evaluated under two operating modes: batch and solvent circulation. Key variables measured include the solvent flow rate (40–160 mL/min), operating temperature (30–50°C), and sweep gas flow rate (100–300 mL/min). The results indicate that under continuous operation with a solvent flow rate of 160 mL/min, a temperature of 30°C, and a sweep gas flow rate of 100 mL/min, 50.42% of the CO<sub>2</sub> was successfully removed. In contrast, the batch system, under identical conditions achieved only a 27.8% removal rate. The superior performance in circulation mode is attributed to the continuous renewal of the solvent, which sustains a stable concentration gradient and minimizes mass transfer resistance. These findings underscore the potential of membrane-based systems with optimized solvent circulation for efficient and stable CO<sub>2</sub> capture in industrial applications.

**Keywords:** carbon dioxide; diethanolamine; membrane contactor; solvent circulation

## 1. Introduction

Natural gas is a major energy resource that plays a significant role to fulfilling global energy demand. It is widely used as a fuel in power plants, various energy generation facilities, and for household needs (Rahmawati et al., 2023). Its strategic role of natural gas as a transitional energy source positions it a key component in addressing the growing global energy demand while reducing carbon emissions. However, natural gas typically contains impurities such as carbon dioxide (CO<sub>2</sub>), which can cause pipeline corrosion, increase maintenance costs, and reduce the calorific value of the gas (Santallum et al., 2021; Ng et al., 2024). Therefore, the removal of CO<sub>2</sub> is essential to ensure the safe, efficient, and sustainable use of natural gas.

A widely studied method for CO<sub>2</sub> separation is absorption, a process in which gas is captured by binding it to a liquid absorbent, typically in the presence of a solvent (Nyamiati et al., 2023). Absorption is generally classified into two types: physical absorption and chemical absorption (Sussatrio et al., 2024). Beyond absorption, other CO<sub>2</sub> separation techniques include adsorption and physical separation methods, such as cryogenic separation and membrane technology (Madejski et al., 2022). Within this context, the membrane contactor emerges, the membrane contactor emerges as a promising alternative to conventional absorption methods. It enables the transfer of acid gases into

the absorbent solvent through a porous structure that enhances mass transfer efficiency. Compared to alkanolamine-based absorption processes, membrane contactors offer significantly lower energy consumption. Moreover, they provide several distinct advantages: they are lightweight, compact, and modular; offer a high surface-area-to-volume ratio; and require a relatively low initial capital investment (Ibrahim et al., 2018).

In the context CO<sub>2</sub> capture, gas-liquid membrane-based contactor have been applied in a variety of module designs and configurations. Membrane contactors categorized into two operational models: parallel and cross-flow. The configuration of flow in gas membranes plays a critical role in determining the efficiency of the separation process. (Scholes & Shen, 2018). A study has been carried out by (Ng et al., 2024) focused on modelling hollow fiber-based membrane contactors featuring two configurations: crossflow and parallel. The results obtained show that the increasing the percentage of cross-flow to the configuration, the more CO<sub>2</sub> gas is absorbed. In 2017, Chang, et al. simulated a cross-flow membrane system designed to handle the concurrent absorption and desorption processes of CO<sub>2</sub> gas. The results obtained show that the cross-flow membrane configuration offered higher efficiency, with more consistent mass flux in several parts of absorption and stripping.

A study by Chavan et al., (2021) focused on membrane contactors for separating CO<sub>2</sub> from N<sub>2</sub> and H<sub>2</sub> mixtures with a 35/65% volumetric ratio. Using a polypropylene membrane and the pH swing absorption method, the study demonstrated a promising recovery of N<sub>2</sub> and H<sub>2</sub>. However, a limitation of this research was the requirement for large tanks, as the absorption and desorption processes do not occur in a single location. Studied conducted by Chang et al., (2017) and Sohaib et al., (2020) explored the simultaneous separation of CO<sub>2</sub> gas through absorption and desorption mechanisms using a hybrid membrane contactor, as well as the use of ionic liquids for concurrent CO<sub>2</sub> capture. Although this method is capable of separating CO<sub>2</sub>, its efficiency level remains relatively lower compared to conventional chemical absorption processes.

The simultaneous absorption and desorption of CO<sub>2</sub> using a novel hybrid membrane contactor (HASMCM) that combines parallel-type and contiguous-type module configurations was the focus of a study conducted by Pan et al in 2017 Propylene carbonate was used as the physical solvent in this study to assess CO<sub>2</sub> capture performance using both simulation and experimental methods. Although the hybrid configuration demonstrated a higher absorption flux compared to conventional single-mode absorption systems, its overall efficiency remains limited. due to the relatively lower performance in low-concentration CO<sub>2</sub> conditions when compared to traditional chemical absorption methods.

The membrane contacts technique employs a hydrophobic microporous membrane to as a stable interface that separates the gas and liquid phases. This facilitates mass transfer while avoiding direct mixing. In Figure 1, the transfer of CO<sub>2</sub> takes place in three distinct stages. The initial step involves the gas from the main stream diffusing to the outer surface of the membrane, followed by its passage through the membrane's porous structure, and ultimately enters the liquid phase. Next, in Figure 2, desorption takes place, during which the bound CO<sub>2</sub> is released by a sweep gas (typically N<sub>2</sub>) through the membrane pores to regenerate the solvent. (Waseem et al., 2025).

The overall mass balance for the simultaneous CO<sub>2</sub> absorption–desorption process can be derived based on the flow diagram presented in Figure 3. This process involves two main phases: the gas phase (feed gas), the liquid phase (solvent), the product gas (sales gas). Assuming steady-state conditions and no mass accumulation within the system, the total mass balance equation can be written as follows.

$$OMB = input - Output \quad (1)$$

$$OMB = Feed + SG_{in} - Sales - L_{out} \quad (2)$$

Next, the mass balance for the CO<sub>2</sub> component, as the target component in this separation process, can be written as follows:

$$In = F \times X_f + L_{in} \times X_{L_{in}} \quad (3)$$

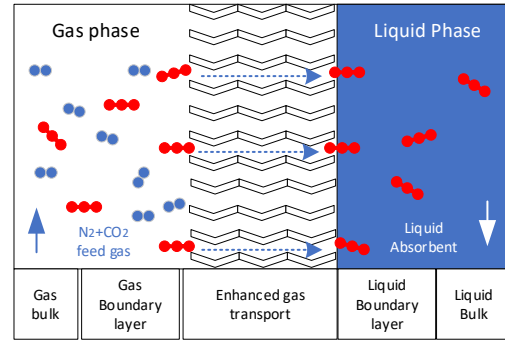


**Figure 1.** The transport behavior of CO<sub>2</sub> during absorption across a porous membrane system

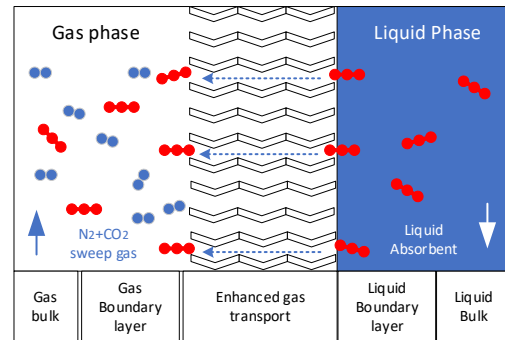


**Figure 2.** Mechanism of CO<sub>2</sub> gas mass transfer in the desorption process on a porous membrane

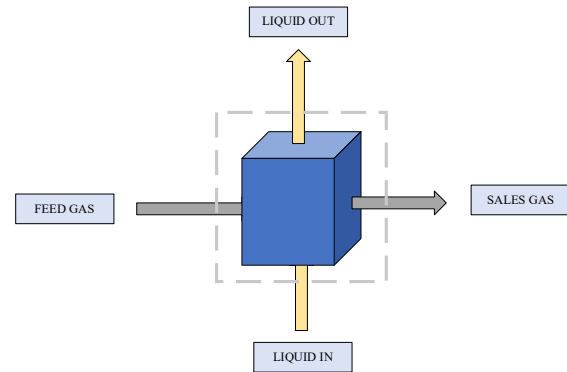


**Figure 3.** Flow Diagram of the Porous Membrane Unit designed for Concurrent Absorption and Stripping Process of Carbon Dioxide

$$Out = Sales \times X_{sales} - L_{out} \times X_{L_{out}} \quad (4)$$

Assuming the system operates under a equilibrium condition, solvent capacity is not a limiting factor, and there is no accumulation of CO<sub>2</sub> in the solvent. Thus, the mass balance equation becomes:

$$F \times X_f = Sales \times X_{sales} \quad (5)$$

Therefore, the calculation of CO<sub>2</sub> removal efficiency can use the equation:

$$\eta = \frac{CO_{2in} - CO_{2out}}{CO_{2in}} \times 100\% \quad (6)$$

To find the absorption flux, an equation can be used that is derived from the energy balance equation in the research equipment system. The absorption flux equation can be seen in the following equation.:

$$(J_{CO_2})_{Abs} = \frac{(Q_{gas\ in} \times C_{gas\ in}) - (Q_{gas\ out} \times C_{gas\ out})}{A_{Abs}} \quad (7)$$

where  $J_{CO_2}$  is the absorption flux ( $\text{mol/m}^2\text{s}$ ),  $Q_{in}$  and  $Q_{out}$  are the flow rates of incoming and outgoing  $CO_2$  gas ( $\text{m}^3/\text{s}$ ),  $C_{in}$  and  $C_{out}$  indicates the amount of carbon dioxide present in the incoming and outgoing gas line ( $\text{mol/m}^3$ ). Meanwhile, to find the value of the desorption flux, the desorption flux equation is used as follows:

$$(J_{CO_2})_{Des} = \frac{(Q_{Sweep\ gas\ out} \times C_{Sweep\ gas\ out})}{A_{Des}} \quad (8)$$

Where  $C_{Sweep\ gas\ out}$  is the concentration of sweep gas and  $Q_{Sweep\ gas\ out}$  is the flow rate of sweep gas.

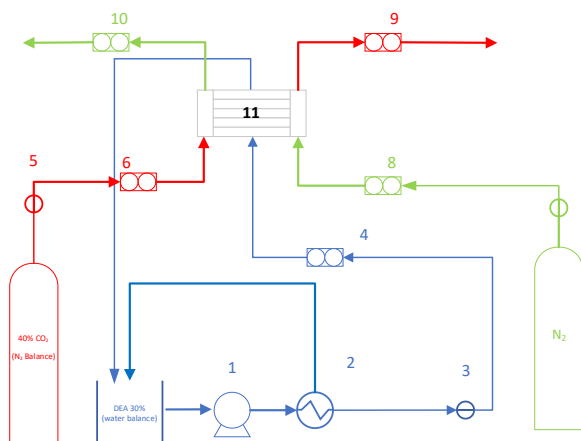


**Figure 4.** Research Equipment Diagram, 1. Pump, 2. Heater, 3. Pressure gauge, 4. Liquid flowmeter, 5. Pressure gauge, 6.  $CO_2$  gas inflow flowmeter, 7. Pressure gauge, 8. Sweep gas inflow glowmeter, 9.  $CO_2$  gas outflow flowmeter, 10. Sweep gas outflow flowmeter, 11. Membrane contactor.

Although numerous studies have been conducted to examine how flow configuration and module design impact the  $CO_2$  absorption and desorption processes utilizing contactor membranes, research specifically highlighting the performance of simultaneous absorption-desorption processes with the addition of continuous flow and variations in solvent flow rates in a double-crossflow membrane configuration remains limited. Several previous studies have focused more on configuration simulations (Chang et al., 2017) or operational stability testing (Chavan et al., 2021), or the implementation of simultaneous absorption-desorption within a hybrid membrane module

using physical solvents (Pan et al., 2017), few have addressed operational factors, such as the influence of solvent circulation systems on process efficiency. The objective of this study is to evaluate the impact of under batch and continuous operating modes in a dual-layer crossflow membrane contactor is the goal of this investigation.

## 2. Materials and Methods

This research uses hydrophobic polypropylene (PP) membrane material obtained from GDP Filter-Indonesia.  $CO_2$  gas was obtained from PT. Aneka Gas Industri Tbk with a concentration entering the membrane module of 40% (balance  $N_2$ ). The solvent used for the  $CO_2$  absorption-desorption process is Diethanolamine (DEA) Merck KGaA 99% diluted to 30% by weight. Other materials required for the chittick titration process are 1 N HCl solution, saturated NaCl solution, NaOH solution, and methyl orange. Here are the specifications of the membrane characteristics to be used as presented in Table 1.

**Table 1.** Characteristics of the membrane constructed from hollow fiber

Parameter	Spesification
Inside diameter	0.35 mm
Outside diameter	0.5 mm
Porous diameter	0.1 $\mu\text{m}$
Fiber Lenght	10 cm
Porosity	0.65 (unitless)
Absorption Area Surface	94.2 $\text{cm}^2$
Desorption Area Surface	904.32 $\text{cm}^2$

### 2.1. Experimental set-up

In this study, a simultaneous absorption-desorption process will be executed using a HFMC with a 30% DEA solvent as the solvent.

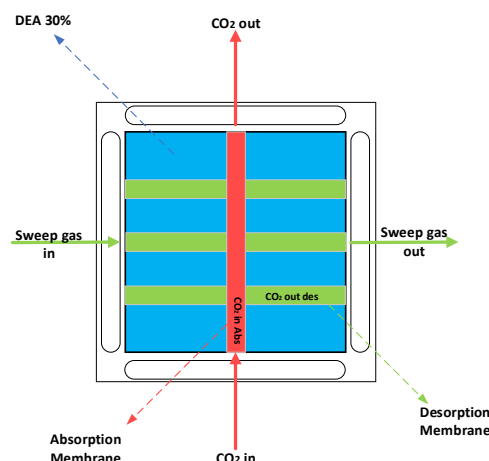


**Figure 5.** Membrane Arrangement Used in the Research

For the gas absorption process, the incoming gas will contain 40%  $CO_2$  and will flow through the membrane tube

in the first layer, while the solvent in the shell will be continuously circulated. Subsequently, a desorption process will also be carried out simultaneously by drawing the incoming CO<sub>2</sub> gas from the second layer tube of the solvent in the shell, where CO<sub>2</sub> will be carried away by the N<sub>2</sub> sweep gas. The layout of the experimental system is presented Figure 4 and Figure 5.

### 3. Results and Discussion

#### 3.1. The Effect of Liquid Flow Rate on Overall Efficiency and Absorption-Desorption Flux

Figure 6 illustrates how variations in liquid flow rate impact the system's overall efficiency. Liquid flow rates used are 40, 80, 120, and 160 mL/min. The observation indicates that a higher the liquid flow correlates with enhanced efficiency. The enhancement in overall efficiency correlates with the intensity of the absorption flux.

Flux is defined as the amount of CO<sub>2</sub> that moves per unit time per unit area of the membrane. The greater the solvent flow rate, the greater the absorption flux, resulting in more CO<sub>2</sub> being absorbed in a given time, thereby reducing the CO<sub>2</sub> in the exit gas. This directly increases the efficiency of the system because more CO<sub>2</sub> from the feed gas is successfully removed. This mechanism aligns with established theory, where the Sherwood number (Sh) representing the ratio of convective to diffusive mass transfer increases with Reynolds number (Re) under laminar flow, indicating improved mass transfer efficiency at higher flow rates. This result is consistent with the research of several researchers such as (Lim et al., 2024) and (Li et al., 2021) reported CO<sub>2</sub> removal efficiencies of around 40–60% at lower liquid flow rates using 2.5 M MEA in a PTFE membrane system.

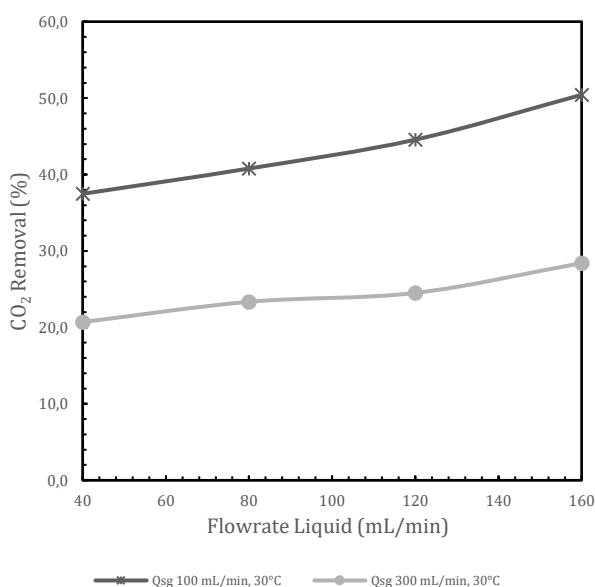


**Figure 6.** Effect of Liquid Flow Rate on Overall Efficiency

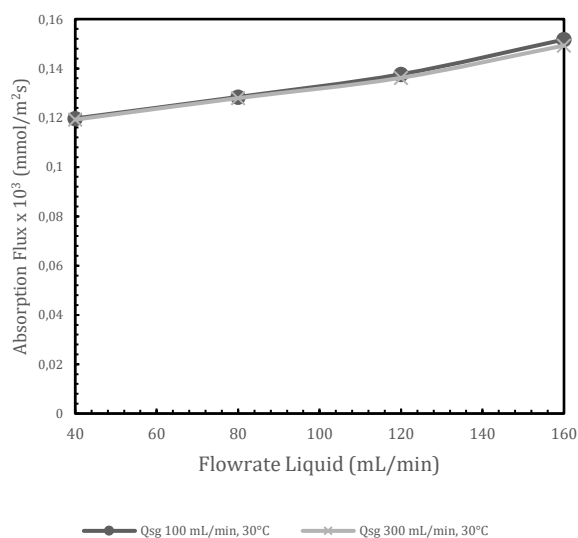
In Figure 7 (a), the data indicates that an increased solvent flow rate significantly enhances the absorption rate. Maximum absorption observed at a flow rate of 160 mL/min. In the absorption process, the feed gas containing a lot of CO<sub>2</sub> passes through the membrane module tube, then diffuses into the solvent through the membrane pores. The transport of CO<sub>2</sub> occurs in three phases: (1) Diffusion of the gaseous component from the bulk phase to the exterior layer of the membrane, (2) penetration through the porous membrane structure up to gas-liquid boundary, and (3) solubility of carbon dioxide into the absorbing liquid. The faster solvent flow rate, the more turbulence in the liquid increases, making the boundary layer thinner, CO<sub>2</sub> gas can transfer from the gaseous stream into the solvent stream thanks to this process.

**Table 2.** Characteristics of the membrane constructed from hollow fiber

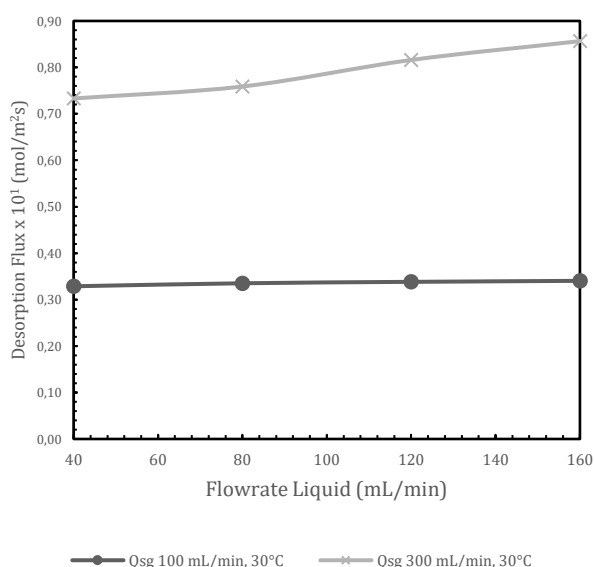
Study	Membrane Type	Solvent	Flow Rate (mL/min)	Absorption flux x 10 <sup>3</sup> (mmol/m <sup>2</sup> s)
Lim et al. (2024)	Polypropilene	MEA (2.5 M)	25–100	0,72
This study	Polypropilene (dual-layer)	DEA (30%)	40–160	0;15

Table 2 compares the absorption flux performance between this study and the work by (Lim et al., 2024). While Lim et al. achieved a maximum absorption flux of 0.72 x 10<sup>3</sup> mmol/m<sup>2</sup>·s using a polypropylene membrane and 2.5 M MEA at flow rates of 25–100 mL/min, this study achieved a flux of 0.15 x 10<sup>3</sup> mmol/m<sup>2</sup>·s using a dual-layer polypropylene membrane and 30% DEA at higher flow rates of 40–160 mL/min. The lower flux observed in this study is attributed to the use of DEA, a weaker base than MEA, which typically shows slower reaction kinetics in CO<sub>2</sub> absorption. However, DEA offers advantages in thermal stability and lower degradation, making it more suitable for long-term and cyclic operation. Furthermore, the use of a dual-layer hollow fiber configuration contributes to maintaining a stable concentration gradient, enhancing process stability even under continuous flow (Li et al., 2021).

Figure 7 (b) illustrates that the desorption flux increases with rising solvent flow rates with the maximum flux observed at a flow rate of 160 mL/min. In the CO<sub>2</sub> desorption process, one of the factors that affects the desorption flux is the solvent flow rate. When this layer is thick, the transfer of trapped CO<sub>2</sub> into the gas phase is hindered. However, when the solvent flow rate increases, this layer becomes thinner, reducing the transfer resistance and resulting in CO<sub>2</sub> being more easily released and diffusing into the gas phase. These findings are consistent with the results reported by (Mohammed et al., 2021) and (Khaisri et al., 2011) who observed desorption flux values ranging from 2.0 to 7.0 × 10<sup>-1</sup> mmol/m<sup>2</sup>·s when using MEA as the solvent at liquid velocities up to 3.5 cm/s



(a)



(b)

**Figure 7.** Effect of Liquid Flow Rate on the Flux of (a) Absorption and (b) Desorption

### 3.2. Overall efficiency, absorption and desorption flux in batch operation

Figure 8 shows the overall efficiency values in the batch operation system with variations in the gas sweep flow rate (Qsg) and temperature. From the graph, it is evident that the highest efficiency is achieved at a Qsg condition of 100 mL/min and a temperature of 30°C. Conversely, the lowest efficiency occurs at a Qsg condition of 300 mL/min and a temperature of 50°C. The decreased contact time between the gas and the solvent at higher gas sweep rates limits the effectiveness of CO<sub>2</sub> mass transfer to the solvent and a drop in efficiency. Additionally, the increase in temperature tends

to decrease the solubility of CO<sub>2</sub> in the solvent negatively affects the solvent's CO<sub>2</sub> absorption capacity to capture CO<sub>2</sub> even though the reaction rate increases. These findings are consistent with results reported by (Aboshatta & Magueijo, 2021).

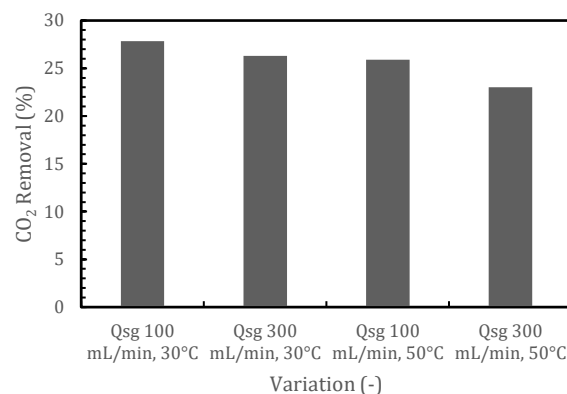
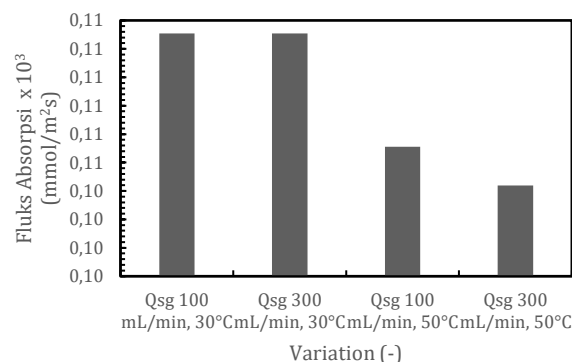
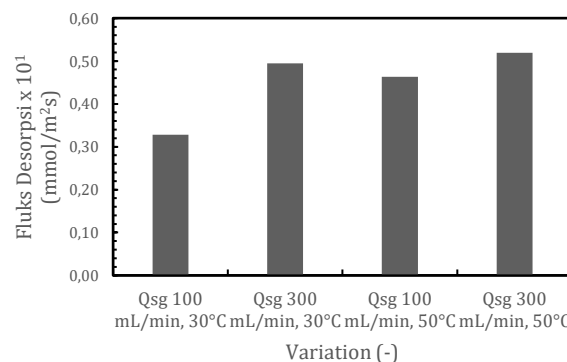


**Figure 8.** Overall Efficiency in Batch Operations

Figure 9 (a) shows the absorption flux values in a batch operation system with variations in sweep gas flow rate (Qsg) and temperature. As shown in the figure the highest flux is achieved at Qsg 100 mL/min and a temperature of 30°C.



(a)



(b)

**Figure 9.** Flux (a) Absorption and (b) Desorption Batch Operation (mmol/m²s) with various sweep gas flow rate

Conversely, the lowest flux occurs at Qsg 300 mL/min and a temperature of 50°C as the absorption process performs optimally at low temperatures. Meanwhile, Figure 9 (b) shows that the desorption flux at 30 °C is notably lower compared to 50°C because desorption occurs optimally at high temperatures. These results are consistent with the research by Aboshatta & Magueijo (2021), which demonstrated that performance in membrane contactor systems.

### 3.3. Comparison of overall efficiency, absorption and desorption flux in circulation and batch operations

Figure 10 presents a comparison of overall CO<sub>2</sub> separation efficiency in the simultaneous absorption-desorption process between batch operation and circulation system with variations in solvent flow rate (QL) from 40 to 160 mL/min. It is evident that the separation efficiency in the batch system exhibits the lowest separation efficiency compared to the circulation system. This is due to the lack of solvent renewal in the batch system, which leads to the gradual saturation of the solvent surface with CO<sub>2</sub> over time.

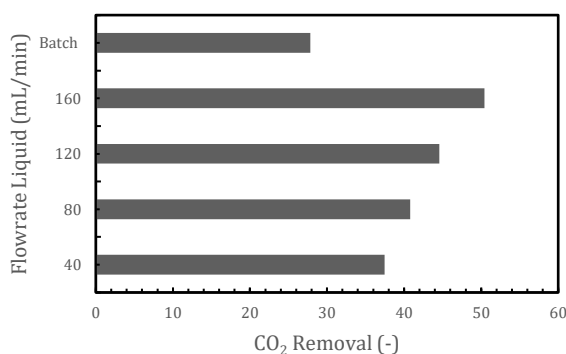
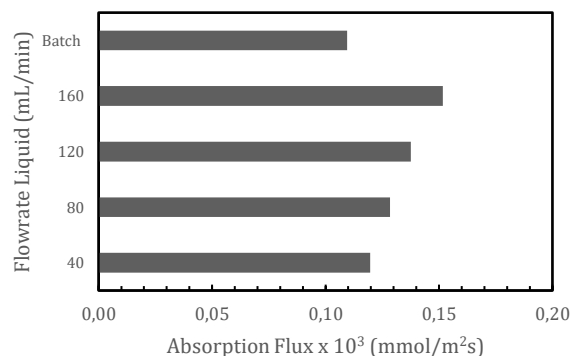


**Figure 10.** Comparison of Overall Efficiency in Batch and Circulation Operations

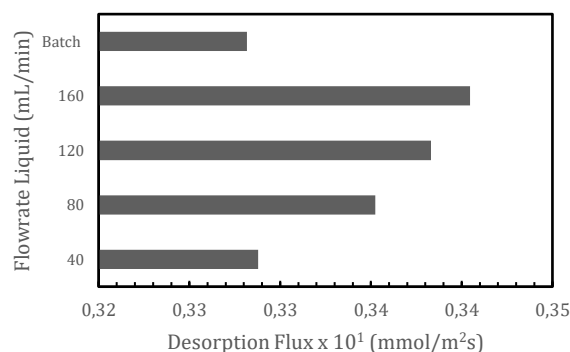
The primary force behind mass transfer, the concentration gradient between the gas and liquid phases, is reduced because of this state. In contrast, in a circulation system, the solvent is continuously renewed, keeping the gas-liquid concentration gradient constant. This contributes to the increased separation efficiency along with the increased solvent flow rate. The higher the circulation rate, the faster the saturated solvent is replaced by fresh solvent, which significantly increases the separation efficiency. This trend is clearly visible from the graph, where efficiency gradually increases as the flow rate rises from 40 mL/min to reach its peak at 160 mL/min. These results are consistent with the research of several researchers such as (Lim et al., 2024) and (Li et al., 2021) reported that higher solvent flow rates enhance CO<sub>2</sub> absorption efficiency in CO<sub>2</sub> absorption efficiency, with a flow rate of 25 to 100 mL/min increasing the efficiency from 50% to 90%.

Figure 11 (a) shows that the CO<sub>2</sub> absorption flux in the batch system is lower compared to the circulation system with various solvent flow rates (40 to 160 mL/min). The flux values in the batch system remain low, indicating limited

mass transfer during the process. A similar trend is observed in Figure 11(b). The CO<sub>2</sub> desorption flux in the batch system is lower compared to the circulation system at various solvent flow rates. This reduced performance is primarily attributed to the lack of continuous solvent flow which leads to the formation of a thick liquid boundary layer near the membrane surface. This layer becomes the main barrier to CO<sub>2</sub> diffusion between the gas and liquid phases because there is no renewal of the solvent on the membrane surface. As a result, the concentration gradient decreases over time, and the mass transfer coefficient also becomes low.



(a)



(b)

**Figure 11.** Comparison of Absorption (a) and Desorption (b) Flux in Batch and Circulation Operations

On the other hand, in a circulation system, the solvent is continuously circulated, resulting in the thinning of the liquid boundary layer. This condition enhances mass transfer by reducing diffusion resistance and maintaining a consistent concentration gradient between the liquid and gas phases. As the flow rate increases from 40 to 160 mL/min, the absorption and desorption fluxes significantly increase, indicating that mass transfer occurs more efficiently. This phenomenon confirms that operations with circulating solvents are superior in maintaining the performance of simultaneous CO<sub>2</sub> absorption and desorption processes, particularly in preventing saturation on the solvent surface and enhancing mass transfer capacity. These findings are consistent with the investigations conducted by (Lim et al., 2024) and (Li et al., 2021) regarding CO<sub>2</sub> absorption, as well as (Mohammed et al., 2021) who used MEA solvent for desorption with a membrane contactor.

#### 4. Conclusions

This research shows that raising the membrane's solvent flow rate significantly enhances separation efficiency and CO<sub>2</sub> flux in the simultaneous absorption–desorption process. The circulation mode of operation exhibited superior performance compared to the batch mode, as continuous solvent renewal helped maintain a stable concentration gradient and reduce mass transfer resistance through boundary layer thinning. Additionally, temperature increase was found to promote the desorption process. Rather than focusing solely on numerical results, these findings demonstrate the potential of membrane-based CO<sub>2</sub> capture systems with optimized solvent circulation for industrial applications, particularly in processes that require operational stability and energy efficiency. This study also lays the groundwork for future research, which could include investigating alternative amine solvents, or incorporating absorption-enhancing elements such as amino acid to further improve performance.

#### Acknowledgments

This research is supported by the Directorate of Research, Technology and Community Service, Ministry of Education, Culture, Research and Technology in accordance with the Master Contract for the implementation of the State University Operational Assistance Program for Master Thesis Research. Master Contract Number: 0419/C3/DT.05.00/PL/2025, dated May 28, 2025. Researcher Contract Number: 1147/PKS/ITS/2025, dated June 3, 2025.

#### Credit authorship contribution statement

**Raditya Yudhi Pamungkas:** Writing: review and editing, writing: initial draft, conceptualization, formal analysis, resources, visualization, validation, and investigation. **Yeni Rahmawati:** Formal analysis, resources, writing, review, and editing; conceptualization; validation. **Siti Nurkhamidah:** Visualization, Project Management, Resources, and Validation. **Fadlilatul Taufany:** Ideas, Materials, Obtaining Funds, and Oversight. **Ali Altway:** Resources, Conceptualization, and Validation. **Susianto:** Data curation, validation, supervision, and methodology.

#### References

- Aboshatta, M., & Magueijo, V. (2021). A Comprehensive Study of CO<sub>2</sub> Absorption and Desorption by Choline-Chloride/Levulinic-Acid-Based Deep Eutectic Solvents. *Molecules*, 26(18), 5595. <https://doi.org/10.3390/molecules26185595>
- Chang, H., Gan, H. Y., Chen, Y. H., & Ho, C. D. (2017). Computational fluid dynamics simulation study of a novel membrane contactor for simultaneous carbon dioxide absorption and stripping. *Energies*, 10(8), 1136. <https://doi.org/10.3390/en10081136>
- Chang, H., Gan, H. Y., Pan, R. H., & Ho, C. D. (2017). CFD Study of Hybrid Membrane Contactors for Absorption and Stripping of Carbon Dioxide. *Energy Procedia*, 105, 4065–4071. <https://doi.org/10.1016/j.egypro.2017.03.859>
- Chavan, S. R., Perré, P., Pozzobon, V., & Lemaire, J. (2021). CO<sub>2</sub> absorption using hollow fiber membrane contactors: Introducing ph swing absorption (phsa) to overcome purity limitation. *Membranes*, 11(7), 496. <https://doi.org/10.3390/membranes11070496>
- Ibrahim, M. H., El-Naas, M. H., Zhang, Z., & Van Der Bruggen, B. (2018). CO<sub>2</sub> Capture Using Hollow Fiber Membranes: A Review of Membrane Wetting. In *Energy and Fuels*, 32(2), 963–978. *American Chemical Society*. <https://doi.org/10.1021/acs.energyfuels.7b03493>
- Khaisri, S., deMontigny, D., Tontiwachwuthikul, P., & Jiratananon, R. (2011). CO<sub>2</sub> stripping from monoethanolamine using a membrane contactor. *Journal of Membrane Science*, 376(1–2), 110–118. <https://doi.org/10.1016/j.memsci.2011.04.005>
- Li, M., Zhu, Z., Zhou, M., Jie, X., Wang, L., Kang, G., & Cao, Y. (2021). Removal of CO<sub>2</sub> from biogas by membrane contactor using PTFE hollow fibers with smaller diameter. *Journal of Membrane Science*, 627. <https://doi.org/10.1016/j.memsci.2021.119232>
- Lim, H., Kim, K., Kim, J., Park, H. S., Kang, J. H., Park, J., & Song, H. (2024). Experimental study of hollow fiber membrane contactor process using aqueous amino acid salt-based absorbents for efficient CO<sub>2</sub> capture. *Journal of Environmental Chemical Engineering*, 12(5). <https://doi.org/10.1016/j.jece.2024.113338>
- Madejski, P., Chmiel, K., Subramanian, N., & Kuś, T. (2022). Methods and Techniques for CO<sub>2</sub> Capture: Review of Potential Solutions and Applications in Modern Energy Technologies. In *Energies*, 15(3). <https://doi.org/10.3390/en15030887>
- Mohammed, H. N., Ahmed, S. M. R., Al-Naseri, H., & Al-Dahhan, M. (2021). Enhancement of CO<sub>2</sub> desorption from MEA-based nanofluids in membrane contactor: Simulation study. *Chemical Engineering and Processing - Process Intensification*, 168. <https://doi.org/10.1016/j.jcep.2021.108582>
- Ng, E. L. H., Lau, K. K., & Lock, S. S. M. (2024). Modelling of carbon dioxide absorption in hollow fiber membrane contactor for different flow configurations. *Results in Engineering*, 24. <https://doi.org/10.1016/j.rineng.2024.103393>
- Nyamiati, R. D., Nurkhamidah, S., Nanda, D. E., Timotius, D., Mahreni, M., Handayani, D. P., Amalia, D., & Krisnabudhi, A. (2023). Current Research on The Development of Carbon Separation and Capture with Polymeric Membrane: A State-of The Art Review. *Eksergi*, 20(2), 58. <https://doi.org/10.31315/e.v20i2.9096>
- Pan, R. H., Chen, Y. R., Tung, K. L., & Chang, H. (2017). Experimental and simulation study of a novel hybrid

- absorption and stripping membrane contactor for carbon capture. *Journal of the Taiwan Institute of Chemical Engineers*, 81, 47–56.  
<https://doi.org/10.1016/j.jtice.2017.10.009>
- Rahmawati, Y., Ariq Sungkono, S., Hawali, Z., Taufany, F., Nurkhamidah, S., & Altway, A. (2023). Performance Test Membrane Contactor for CO<sub>2</sub> Desorption from DEA. In *The Journal of Engineering*, 9(1).  
<https://doi.org/10.12962/j23378557.v9i1.a16642>
- Santallum, E. M., Tibalia, E., Hemawati, F., Kristiana, V., Prima, G., & Budianto, I. (2021). Modifikasi Zeolit Alam Menjadi ZSM-5 Sebagai Penjerap CO<sub>2</sub> Modification of Natural Zeolite to ZSM-5 as CO<sub>2</sub> Adsorber, *Eksergi*, 18(2).  
<https://doi.org/10.31315/e.v18i2.4725>
- Scholes, C. A., & Shen, S. (2018). Mass transfer correlations for membrane gas-solvent contactors undergoing carbon dioxide desorption. *Chinese Journal of Chemical Engineering*, 26(11), 2337–2343.  
<https://doi.org/10.1016/j.cjche.2018.05.005>
- Shimada, K., Seekkuarachchi, I. N., & Kumazawa, H. (2006). Absorption of CO<sub>2</sub> into aqueous solutions of sterically hindered methyl aminoethanol using a hydrophobic microporous hollow fiber contained contactor. *Chemical Engineering Communications*, 193(1), 38–54.  
<https://doi.org/10.1080/009864490923484>
- Sohaib, Q., Vadillo, J. M., Gómez-Coma, L., Albo, J., Druon-Bocquet, S., Irabien, A., & Sanchez-Marcano, J. (2020). CO<sub>2</sub> capture with room temperature ionic liquids; coupled absorption/desorption and single module absorption in membrane contactor. *Chemical Engineering Science*, 223.  
<https://doi.org/10.1016/j.ces.2020.115719>
- Sussatrio, H., Hadiyanto, H., & Widayat, W. (2024). Optimasi Komposisi MDEA dan MEA Sebagai Absorbent untuk Proses Penghilangan CO<sub>2</sub> dalam Produksi Gas di Lapangan A. *Eksergi*, 21(1), 29.  
<https://doi.org/10.31315/e.v21i1.10855>
- Waseem, M., Ghasem, N., & Al-Marzouqi, M. (2025). Advances in hollow fiber membrane contactors for CO<sub>2</sub> stripping. In *Materials Today Sustainability*, 29.  
<https://doi.org/10.1016/j.mtsust.2024.101056>